Published in final edited form as:
Nanomedicine. 2014 January ; 10(1): . doi:10.1016/j.nano.2013.07.003.

Convection enhanced delivery and *in vivo* imaging of polymeric nanoparticles for the treatment of malignant glioma

Giovanna M Bernal, PhD[#a], **Michael J LaRiviere, BS**[#a], **Nassir Mansour, MD**[a], **Peter Pytel, MD**[b], **Kirk E Cahill, BS**[a], **David J Voce, BS**[a], **Shijun Kang, MD**[a], **Ruben Spretz, PhD**[c], **Ulrich Welp, PhD**[d], **Sandra E Noriega, PhD**[c], **Luis Nunez, PhD**[c], **Gustavo F Larsen, PhD**[c], **Ralph R. Weichselbaum, MD**[e], and **Bakhtiar Yamini, MD**[a]

[a]Section of Neurosurgery, Department of Surgery, Pritzker School of Medicine, The University of Chicago, Chicago, Illinois, USA

[b]Department of Pathology, Pritzker School of Medicine, The University of Chicago, Chicago, Illinois, USA

[c]Biotarget Inc. and LNK Chemsolutions LLC, Lincoln, Nebraska, USA

[d]Material Science Division, Argonne National Laboratory, Argonne, Illinois, USA

[e]Department of Radiation and Cellular Oncology, Pritzker School of Medicine, The University of Chicago, Chicago, Illinois, USA

[#] These authors contributed equally to this work.

Abstract

A major obstacle to the management of malignant glioma is the inability to effectively deliver therapeutic agent to the tumor. In this study, we describe a polymeric nanoparticle vector that not only delivers viable therapeutic, but can also be tracked *in vivo* using MRI. Nanoparticles, produced by a non-emulsion technique, were fabricated to carry iron oxide within the shell and the chemotherapeutic agent, temozolomide (TMZ), as the payload. Nanoparticle properties were characterized and subsequently their endocytosis-mediated uptake by glioma cells demonstrated. Convection enhanced delivery (CED) can disperse nanoparticles through the rodent brain and their distribution is accurately visualized by MRI. Infusion of nanoparticles does not result in observable animal toxicity relative to control. CED of TMZ bearing nanoparticles prolongs the survival of animals with intracranial xenografts compared to control. In conclusion, the described nanoparticle vector represents a unique multifunctional platform that can be used for image-guided treatment of malignant glioma.

Keywords

Nanoparticle; glioma; MRI; convection

INTRODUCTION

There are over 22,000 new cases of primary malignant brain tumors diagnosed in the United States each year.[1] Despite standard multimodal treatment, median survival remains about

Address correspondence to: Bakhtiar Yamini, MC 3026, Section of Neurosurgery, 5841 S. Maryland Ave, University of Chicago Hospitals, Chicago, IL, 60637, USA. Phone: (773) 702-4452; Fax: (773) 702-3518; byamini@surgery.bsd.uchicago.edu.

Conflicts of Interest: Biotarget Inc. and LNK Chemsolutions LLC have commercial interests in the particle systems described in this work.

one year and local tumor recurrence is virtually universal.[2, 3] The addition of chemotherapy to surgery and ionizing radiation (IR) improves patient survival,[4] suggesting that better therapeutic delivery can make a significant impact to overall patient prognosis. To improve intracranial delivery, chemotherapeutic concentrations may be increased or the blood brain barrier (BBB) temporarily opened. While such techniques increase the killing of tumor cells, they also result in an increase in normal tissue toxicity. Direct intratumoral implantation of drug (e.g. using impregnated polymers) can bypass the BBB, but agent distribution is limited by its ability to diffuse through the tissue. Convection enhanced delivery (CED) is a direct delivery method that uses a hydrostatic pressure gradient to distribute macromolecules through the brain tissue via catheters implanted during surgery.[5, 6]

CED can significantly increase the volume of distribution (V_d) of infused macromolecules. However, several studies, including a recent clinical trial,[7] highlight the unpredictable nature of agent distribution by CED.[8] Loss of infusate into the ventricles and subarachnoid space or the anisotropic tissue surrounding a tumor all contribute to the random nature of agent dispersal.[9, 10] This unpredictable pattern is seen despite optimal catheter placement. In an attempt to overcome the limitation of random distribution, real-time or post-infusion imaging can be used. Such an approach enables mid-procedure adjustments, or additional treatments, to be made to target areas not initially covered. This treatment paradigm, referred to as adaptive image guidance, is used extensively with radiation therapy of non-central nervous system tumors.[11]

The development of new therapies for the management of malignant glioma has accentuated the need for a vector system to effectively deliver these agents. A model vector is biocompatible, non-toxic and stable in the tumor microenvironment. The ability to be imaged is an additional attribute that has become more important as the first generation of vectors has been tested clinically. Vector systems are generally divided into two groups: viral and non-viral. Although viral vectors have received the most attention, they suffer from significant drawbacks, such as their potential toxicity, difficulty with large-scale production and inability to incorporate MRI contrast agents.[12] Among non-viral vectors, liposomes have had some clinical use in the delivery of chemotherapeutics.[13] Nevertheless, no system has stood out as being significantly better than another in the management of malignant glioma.

Polymeric nanoparticles (NPs) are compelling for use as multi-dimensional vehicles because not only can they deliver a therapeutic payload, but they can also be fabricated to incorporate an MRI contrast agent for real-time imaging. To date, convection of nanoparticles has not been well studied, and the stringent requirements necessary for NP dispersion by CED,[14, 15] mean that each NP system needs to be systematically tested and modified in order to optimize their distribution in the brain. In this study, we report the production of a polymeric NP vector containing iron oxide and loaded with the anti-glioma agent, temozolomide (TMZ). These NPs, fabricated specifically for CED, can be convected through the rodent brain and tracked *in vivo* by standard MR imaging. Furthermore, TMZ-encapsulating NPs are shown to effectively reduce the growth of glioma xenografts and extend survival of tumor bearing animals.

METHODS

Animals and cells

Six- to 7-week-old male Lewis rats or male athymic nude mice (Harlan Laboratories, Indianapolis, IN) were used as described below. Surgery was performed in accordance with the guidelines of the Institutional Animal Care and Use Committee of the University of Chicago to provide humane care of these animals. The human glioblastoma cell line, U87

MG, was acquired from the American Type Culture Collection (ATCC) and cultured as previously described.[16]

Polymeric magnetite-bearing NP (PMNP) fabrication and characterization

PMNPs were produced using a proprietary electrohydrodynamic technology (Bio-Target Inc. and LNK Chemsolutions LLC, USA). Briefly, for all NP formulations, organic solutions containing all the necessary components were processed using this technology resulting in a dry collection of the specified nanoparticles. The collected material was then harvested in an aqueous buffer solution to obtain a stable suspension. The NP formulations used include: 1) Blank PMNPs (particles containing only polymers and magnetite); 2) Fluorescent PMNPs (same composition as Blank PMNPs, with either rhodamine or fluorescein); and 3) TMZ-containing PMNPs (same components as Blank PMNPs, plus fluorescein and TMZ). PMNPs were suspended in a 2:2:1 solution of 1% (w/v) BSA, pH 7.4 PBS and sterile water, respectively. For payload release, PMNPs were suspended in 0.25% Tween-20 in pH 7.4 PBS solution, to avoid BSA interference in the UV-Vis analysis. Centrifugation was performed at 9,500 g for 4 min to isolate sub-100 nm particles from the crude fraction. For dynamic light scattering (DLS) analysis, PMNPs were diluted 1:20 in PBS and a Zetasizer Nano ZS (Malvern, Worcestershire, UK) was used. For Transmission electron microscopy (TEM) studies, a TEM JEOL model 1220 at 120kV was used. Magnetic susceptibility experiments were carried out on a Superconducting Quantum Interference Device (SQUID) with dry pellets of 1/8×, 1/2x, 1×, and 2× PMNPs (where x= a magnetite concentration of 13.2 μg/μl). Magnetic fields ranging from −5 to +5T were used, as this range includes field strengths found in common human and animal MRI scanners.

For examination of *in vitro* release kinetics, 100 mg of as-collected nanoparticles were suspended in 10 ml of 0.25% PBS-Tween Buffer (pH=7.4). Since TMZ is only stable at acidic pH in aqueous solution, the history of TMZ released from the particles would be masked if the TMZ present in solution is included in the quantification. To solve this problem, only TMZ protected inside the particles is quantified after separating the particles from the liquid in the suspension and then chemically disrupting the polymers by adding 100 μl of HCl 0.1 N. Once the polymer in the nanoparticles was completely disrupted, the supernatant was separated and TMZ quantified by UV-Vis spectroscopy (HP 8452 A Diode Array Spectrophotometer) following the absorbance at 330 nm wavelength that corresponds to the aromatic ring carbonyl group of TMZ n-γ electronic transition.[17] At t=0, the amount of TMZ quantified is the total initial TMZ content in the particles. At any other time in suspension, an aliquot can be isolated, particles separated and disrupted, and its TMZ content quantified as above. The TMZ released from the particles into the solution up to that time, regardless of decomposition in aqueous solution, is determined by subtracting the measured amount in the particles at the given time from the total initial amount of TMZ. Release studies were performed at 4°C, 22°C and 37°C and all measurements performed in duplicate.

PMNP uptake

For uptake quantification studies, U87 cells were pretreated with either 30 nM chlorpromazine (Sellekchem Inc, Houston, TX) or 450 mM sucrose for 30 minutes prior to nanoparticle administration. The indicated volume of PMNPs was added to cells in 2.5 ml of media and kept in the same media containing the inhibitors for two hours prior to analysis using a FACSort instrument (Becton Dickinson Immunocytometry Systems, San Jose, CA). For fluorescence microscopy studies, U87 cells were plated overnight and then incubated with either 1 μl of rhodamine-tagged PMNPs or rhodamine in media for two hours. Cells were then rinsed twice and fixed for 10 min with formalin. Following two more rinses, each well was coverslipped using ProLong Gold with DAPI nuclear stain (Invitrogen, Carlsbad,

CA). Cells were then visualized with Olympus DSU Spinning Disk Confocal microscope using an Evolve back-thinned CCD camera.

CED and PMNP distribution

CED was performed using a step-design catheter similar to one previously described.[18] Briefly, the catheter was made of fused silica tubing (167 μm OD and 100 μm ID) attached to a 26 gauge needle connected via PEEK tubing to a 250 μL Hamilton syringe (Reno, NV) and powered by a BASi syringe pump (West Lafayette, IN). For distribution experiments, rats were placed in a Kopf stereotactic frame to target the right striatum (1.0 mm AP, 3.0 mm L, and 6.0 mm Ventral to bregma). The catheter was slowly lowered and after 5 minutes, 25 μl of NPs infused at a rate of 0.5 μL/min. The catheter was then slowly retracted and animals recovered. Bolus injections were performed using the same catheter system at an infusion rate of 25 μL/min.

In vivo MRI

PMNPs or PNPs were infused via either CED or bolus and animals placed in the MRI scanner within 1 hour of infusion termination. T2-weighted MR images were acquired using a 9.4T GE MRI and a low pass birdcage RF coil. T2-weighted fast spin echo MR images were acquired with a 256× 256 matrix, TR/TE 300/4.1 to 701/2.7 ms, echo time of 64 ms, and 0.5 mm slices with no gap. Animals were sacrificed immediately following MRI acquisition and images analyzed with OsiriX (Pixmeo, Geneva, Switzerland).

Histology

Rats were sacrificed immediately after infusion, or in some cases after MRI, and the brains removed, fixed in OCT (Sakura Finetek USA Inc., Torrance, California) and sectioned at 20 μm with a cryostat. For fluorescently-tagged NPs, sections were examined at low power with a FITC filter, and images analyzed using ImageJ (NIH). For analysis of general brain histology and for determination of iron oxide distribution, formalin fixed brains were sectioned and then stained with either hematoxylin and eosin or Prussian blue dye, respectively.

Calculation of V_d/V_i

To calculate and compare the volume of distribution to volume of infusion (V_d/V_i) ratio between bolus and CED infusions, serial images displaying the infusion site were identified using ImageJ (NIH) and the region of either hypointensity (MRI) or fluorescence (fluorescence imaging) selected. The cross-sectional area of signal for each section was calculated using the known section thickness (defined as the distance between consecutive cryostat sections), and summed across serial sections to obtain V_d. The V_d was then divided by the volume of infusate administered (V_i). Backflow, dorsal to the corpus callosum, was excluded from the volume measurements in both CED and bolus infusion.

In vivo glioma studies

Hind limb experiments—For hind limb experiments, 5×10^6 U87 cells in a 100 μL suspension were inoculated into the right hind limb muscle of nude mice and tumor size measured daily with calipers. When tumors reached an average size of 200 mm^3, animals were randomized into four groups and treatment started (day 0). For all treatments, the respective PMNP formulations were injected intratumorally on day 0, 3 and 5. Treatment groups included: i) untreated control (UTC), ii) blank-NPs (no TMZ), iii) TMZ-loaded NPs (TMZ equivalent concentration was 5 mg/kg/dose), and iv) the supernatant acquired after filtering TMZ-loaded PMNPs through a 10 nm filter. Fractional tumor volume, relative to day 0 for each individual animal, was plotted every 2-3 days.

Intracranial experiments—5×10^5 U87 cells were inoculated into the right striatum as previously described.[16] On day 4 and 7 after tumor grafting, animals were treated with 10 μl of the indicated PMNPs infused by CED intracranially to the same coordinates as the tumor. Mice were monitored daily and sacrificed when they displayed signs of terminal disease.

Statistical analysis

Results are expressed as mean ± SD. Statistical significance was taken as $P < 0.05$, using 2-tailed Student's *t*-test. Kaplan-Meier survival curves were plotted for the intracranial experiment and analyzed by the log-rank method.

RESULTS

Development and characterization of optimal PMNPs for CED through the brain

In designing NPs for use against malignant glioma, a polymer system composed of a mixture of functionalized polyethylene glycol (PEG), polylactide (PLA), and polycaprolactone (PCL) was used. Such a polymer enables formation of <100 nm diameter NPs with a negative surface charge, two properties that allow for robust convection through the extracellular space of brain parenchyma.[14] Additionally, PEG-PLA-PCL was chosen as it can incorporate a variety of compounds within the polymer on forming NPs. Superparamagnetic iron oxide (magnetite) was incorporated into the NP shell to produce PMNPs (Figure 1A). At each stage in NP development, the ratio of the components was systematically adjusted to optimize encapsulation, drug delivery and imaging. Both Dynamic light scattering (DLS) studies (Figure 1B) and transmission electron microscopy (TEM; Figure 1C) reveal that NPs have a diameter of <100 nm, and a slightly negative surface charge (zeta, ζ, potential = −7.75 mV; data not shown). Magnetic susceptibility measurements reveal that an increase in iron oxide concentration results in an increase in magnetic susceptibility in fields up to 5 Tesla (Figure 1D), confirming the superparamagnetic property of the NPs. PMNPs with 11 % iron oxide content were found to offer the best balance between polymer content and magnetic susceptibility. Finally, TMZ release was determined using UV-Vis spectroscopy. At 37°C, complete release of payload (TMZ) is achieved after approximately 20 hours, while at lower temperatures PMNPs are more stable with a slower release profile (Figure 1E). These data indicate that PMNPs have characteristics that are compatible with CED and, while stable when refrigerated, PMNPs release their payload more quickly at physiological temperature.

CED efficiently distributes PMNPs in the rat brain

A rat model was used to examine CED through the brain. Using a step design catheter system,[18] fluorescein-tagged PMNPs were infused into the striatum of Lewis rats either via CED or bolus injection (Figure 2A). Fluorescence microscopy of histological specimens reveals that CED results in significantly higher V_d relative to V_i when compared to the ratio achieved with bolus injection ($P < 0.05$, Figure 2B). Importantly, animals subjected to PMNP infusion do not show any systemic signs of distress or trauma compared to controls.

Next, PMNP dispersion was examined *in vivo* using MRI (Figure 2C). As with fluorescence imaging, MRI studies show that delivery by CED results in a significant increase in PMNP distribution relative to bolus infusion (Figure 2D, $P < 0.05$). Serial T2-weighted images of a representative MR scan demonstrate the presence of hypointense signal centered on the CED infusion site (Figure 2C, white arrows). Bolus injection fails to distribute PMNPs ventral to the catheter tip, resulting instead in PMNP backflow along the catheter tract (Figure 2C, black arrows). The V_d/V_i values calculated on MRI are similar to their respective values as determined by fluorescence microscopy (Figure 2D). Although the hypointense signal seen following PMNP infusion is likely due to the iron oxide, we

confirmed this observation by infusing NPs that do not contain iron oxide. While iron oxide containing PMNPs produce a hypointense MR signal following CED, identical NPs that have no iron oxide (PNPs) do not (data not shown). These findings indicate that CED can effectively distribute PMNPs and that it is specifically the iron oxide in the PMNPs, and not a different factor associated with the infusion, that is visualized by MRI.

Histological examination of rat brains was also performed to analyze both the pathology and distribution of bolus compared to CED administration. Focal, procedure-related hemorrhage, demonstrated by the presence of red blood cells, is observed at the site of catheter insertion following both bolus injection (Figures 3A and B) and CED infusion (Figures 3C and D). While CED results in some local edema, as demonstrated by the mild increase in the extracellular space size in the region of infusion (Figures 3C and D), no gross parenchymal changes are seen following infusion. This observation suggests that convection of PMNPs does not grossly damage the surrounding brain tissue. In addition, PMNP distribution was examined by staining for iron oxide using Prussian blue dye (Figure 3E). CED results in iron oxide distribution distant from the injection site, a finding consistent with the results obtained on MRI and fluorescence imaging.

PMNPs are taken up by glioma cells and deliver effective TMZ

PMNP cellular uptake was initially quantified using FACS analysis of cells incubated with fluorescently-tagged PMNPs. A concentration-dependent increase in nanoparticle uptake is noted within 2 hours of exposure of cells to PMNPs with close to 100 % of cells being positive when 0.5 μl of PMNP are used (Figure 4A, left). In addition, fluorescence imaging demonstrates PMNP uptake specifically in the cytoplasm (Figure 4A, right). Next, to examine the role of endocytosis in PMNP uptake, chlorpromazine (CPZ), a clathirin-mediated endocytosis inhibitor,[19] and hypertonic sucrose solution, a non-selective endocytosis inhibitor,[20] were used. A significant decrease in fluorescence-positive cells is seen following pre-treatment with either CPZ or hypertonic sucrose, especially at low PMNP concentrations (Figure 4B), indicating that PMNP uptake is at least in part endocytosis-mediated. The ability to deliver therapeutic agent was assessed by examining clonogenic survival following exposure of cells to PMNPs loaded with TMZ. TMZ-PMNPs decrease the surviving fraction of U87 cells in a concentration-dependent manner whereas even a high concentration of blank PMNPs does not affect surviving fraction compared to untreated cells (Figure 4C). To examine whether uptake of TMZ-loaded PMNPs is required for this effect, clonogenic survival was examined in the presence of hypertonic sucrose. Hypertonic sucrose has a small effect on clonal survival on its own and does not significantly alter survival following treatment with blank PMNPs (Figure 4D). However, sucrose completely reverses the decrease in colony formation induced by TMZ-PMNPs (Figure 4D). Importantly, these results are not due to hypertonic sucrose altering the integrity of PMNPs themselves as determined by examining PMNPs that were pre-incubated in sucrose prior to use (data not shown). Together, these data suggest that PMNPs need to be taken up by glioma cells and release their therapeutic payload intra-cellularly for the cytotoxic effect.

To assess the anti-glioma effect of TMZ-PMNPs, two animal models of malignant glioma were used. First, U87 glioma xenografts were established in the hind limb of athymic nude mice and tumors treated with a single intra-tumoral injection of TMZ-PMNPs, blank PMNPs, or the supernatant after filtering TMZ-PMNPs. Fractional tumor volume, relative to day 0, was then compared to that of untreated controls (UTC). TMZ-PMNPs significantly reduce tumor growth compared to untreated and those treated with blank PMNPs ($P < 0.05$ at day 20) (Figure 5A). Furthermore, no change in growth is seen following administration

of the filtered supernatant suggesting that TMZ is contained within the PMNPs themselves and not free in the solvent.

Given the critical importance of the local environment in the treatment of malignant glioma, we next examined treatment efficacy using an intracranial glioma model. U87 xenografts were established in the striatum of athymic nude mice and animal survival monitored following CED of TMZ-PMNPs compared to controls. Administration of TMZ-PMNPs significantly extends the survival of xenografted mice when compared to both untreated animals and those treated with blank-PMNPs ($P < 0.03$, Figure 5B). These data indicate that PMNPs can safely deliver effective concentrations of chemotherapeutic agent intracranially and suggest that this system can be used to treat malignant glioma.

DISCUSSION

In the current work, we describe a polymeric nanoparticle vector specifically designed for image-guided treatment of malignant glioma. Nanoparticles were fabricated using a combination of FDA-approved polymers to produce a vector with optimal properties for convection through the brain parenchyma.[15, 21] Specifically, NPs with a diameter less than 100 nm and a negative surface charge were obtained. In addition, NPs were loaded with superparamagnetic iron oxide for MR imaging. These PMNPs were designed to have a core/shell structure that allows them to protect a specific payload in their center (Figure 1A). Although the anti-glioma agent, TMZ, was used as the payload for this work, it is anticipated that a broad range of therapeutics or toxins can be encapsulated and delivered. In initial studies, we characterized the physical properties and payload release profile of PMNPs. Subsequently, CED was employed to disperse PMNPs through rat brains and their distribution pattern examined using MRI. In addition, the ability of PMNPs to be taken up into cells and deliver viable TMZ was examined in cell culture experiments. Finally, after having determined that this vector is safe for use *in vivo*, studies were performed in animal glioma models to demonstrate the efficacy of PMNP as a vector for delivery of chemotherapeutic to the brain.

The BBB represents one of the most important obstacles to the effective treatment of malignant glioma. One technique used to bypass this barrier and deliver adequate levels of therapeutic to glioma cells involves direct intra-parenchymal injection using CED.[6] We demonstrate that PMNPs can be distributed in the brain parenchyma by CED. Although this technique enables a larger V_d than using simple bolus, it is notable that the V_d/V_i of PMNP dispersion is less than 1 (Figure 2). While this distribution ratio is adequate for treatment of an animal model of malignant glioma, some concern is raised for the potential translation of this technique to clinical tumors where tissue characteristics surrounding gliomas will further restrict the ability to adequately cover the tumor. Specifically, the inhomogeneity and anisotropy of glioma-infiltrated brain can yield unpredictable distribution geometry following CED.[22] Indeed, the disappointing results of recent clinical trials using CED can, at least in part, be attributed to insufficient tumor coverage following convection.[23] While infusing greater volumes of PMNPs, for longer periods of time, may improve the overall tumor coverage, it is conceivable that PMNP infusion may be best used to target small regions of residual tumor that remain following surgical debulking.

Given the difficulty with predicting distribution pattern following CED, a significant advantage of PMNPs is the ability to visualize them with standard MRI. As CED is a blind process, real-time and post-operative imaging is essential to confirm that the delivered therapeutic adequately covers the intended target region. In the event of insufficient coverage, the infusion can be redirected or additional infusions performed to enable maximal target coverage. PMNP distribution pattern was demonstrated with MRI and

verified histologically both by fluorescence imaging and iron oxide staining. While it is clear that iron oxide is a useful contrast agent,[24] consideration must also be given to the potential toxicity associated with accumulation of this molecule in the brain. In this regard, it has been reported that uncoated iron oxide NPs can induce reactive oxygen species production, inflammation and DNA damage.[25] However, coating iron oxide with polymers such as PEG has been shown to render PMNPs biocompatible.[26] In the long term, iron oxide crystals are in part metabolized, leading to increased hepatic and splenic ferritin storage, and in part incorporated into red blood cells.[27] While it is reported that iron oxide remains in brain tissue even 3 months after injection, histological data shows no gross pathological findings associated with this accumulation.[28] Moreover, our results show that after 3 weeks, the MRI signal is reduced to less than 25 % of the original (data not shown) and that PMNP infusion is well tolerated with minimal toxicity.

Despite the efficacy of using PMNPs to deliver TMZ *in vivo*, that the actual drug delivery efficiency is quite low. This finding may hinder the potential clinical use of PMNPs. To improve overall delivery, targeting moieties such as antibodies or ligands can be incorporated onto the PMNP surface to increase delivery efficiency as previously reported.[24] Also, increasing the drug concentration within the PMNPs may improve the total amount of agent delivered. Ultimately however, the potential of this system for clinical use will require further examination in higher order animals that have spontaneous tumors such as found in a canine model.[29] It is also possible that PMNPs may be better suited for delivery of other types of therapeutic agents. In this regard, the ability of PMNPs to specifically deliver their payload to the cellular cytoplasm suggests that they may be ideal for delivery of si-RNA that mediates its effect in the cytoplasm.

In conclusion, we present a novel nanoparticle vector that represents a versatile platform that can be used to overcome many delivery-related obstacles associated with treatment of malignant glioma. Importantly, successful intracranial delivery raises the possibility of using such a system not only for treating tumors but also for the management of a broad range of central nervous system diseases.

Acknowledgments

This work was supported by NIH R44CA135906-02 (RS, LN and BY), NIH 1R01CA136937 (BY) and the Ludwig Center for Metastasis Research.

REFERENCES

1. Siegel R, Naishadham D, Jemal A. Cancer statistics, 2012. CA: a cancer journal for clinicians. 2012; 62:10–29. [PubMed: 22237781]
2. Paszat L, Laperriere N, Groome P, Schulze K, Mackillop W, Holowaty E. A population-based study of glioblastoma multiforme. Int J Radiat Oncol Biol Phys. 2001; 51:100–7. [PubMed: 11516858]
3. Hess CF, Schaaf JC, Kortmann RD, Schabet M, Bamberg M. Malignant glioma: patterns of failure following individually tailored limited volume irradiation. Radiother Oncol. 1994; 30:146–9. [PubMed: 8184112]
4. Stewart LA. Chemotherapy in adult high-grade glioma: a systematic review and meta-analysis of individual patient data from 12 randomised trials. Lancet. 2002; 359:1011–8. [PubMed: 11937180]
5. Bobo RH, Laske DW, Akbasak A, Morrison PF, Dedrick RL, Oldfield EH. Convection-enhanced delivery of macromolecules in the brain. Proc Natl Acad Sci U S A. 1994; 91:2076–80. [PubMed: 8134351]
6. Ferguson SD, Foster K, Yamini B. Convection-enhanced delivery for treatment of brain tumors. Expert Rev Anticancer Ther. 2007; 7:S79–85. [PubMed: 18076322]

7. Kunwar S, Chang S, Westphal M, Vogelbaum M, Sampson J, Barnett G, et al. Phase III randomized trial of CED of IL13-PE38QQR vs Gliadel wafers for recurrent glioblastoma. Neuro Oncol. 12:871–81. [PubMed: 20511192]
8. Fiandaca MS, Forsayeth JR, Dickinson PJ, Bankiewicz KS. Image-guided convection-enhanced delivery platform in the treatment of neurological diseases. Neurotherapeutics. 2008; 5:123–7. [PubMed: 18164491]
9. Linninger AA, Somayaji MR, Mekarski M, Zhang L. Prediction of convection-enhanced drug delivery to the human brain. J Theor Biol. 2008; 250:125–38. [PubMed: 17950757]
10. Raghavan R, Brady ML, Rodriguez-Ponce MI, Hartlep A, Pedain C, Sampson JH. Convection-enhanced delivery of therapeutics for brain disease, and its optimization. Neurosurg Focus. 2006; 20:E12. [PubMed: 16709017]
11. Wu QJ, Li T, Wu Q, Yin FF. Adaptive radiation therapy: technical components and clinical applications. Cancer J. 17:182–9. [PubMed: 21610472]
12. El-Aneed A. An overview of current delivery systems in cancer gene therapy. J Control Release. 2004; 94:1–14. [PubMed: 14684267]
13. Hofheinz RD, Gnad-Vogt SU, Beyer U, Hochhaus A. Liposomal encapsulated anti-cancer drugs. Anticancer Drugs. 2005; 16:691–707. [PubMed: 16027517]
14. Allard E, Passirani C, Benoit JP. Convection-enhanced delivery of nanocarriers for the treatment of brain tumors. Biomaterials. 2009
15. Chen MY, Hoffer A, Morrison PF, Hamilton JF, Hughes J, Schlageter KS, et al. Surface properties, more than size, limiting convective distribution of virus-sized particles and viruses in the central nervous system. J Neurosurg. 2005; 103:311–9. [PubMed: 16175862]
16. Yamini B, Yu X, Gillespie GY, Kufe DW, Weichselbaum RR. Transcriptional targeting of adenovirally delivered tumor necrosis factor alpha by temozolomide in experimental glioblastoma. Cancer Res. 2004; 64:6381–4. [PubMed: 15374943]
17. Babu NJ, Sanphui P, Nangia A. Crystal engineering of stable temozolomide cocrystals. Chemistry, an Asian journal. 2012; 7:2274–85.
18. Krauze MT, Saito R, Noble C, Tamas M, Bringas J, Park JW, et al. Reflux-free cannula for convection-enhanced high-speed delivery of therapeutic agents. J Neurosurg. 2005; 103:923–9. [PubMed: 16304999]
19. Rothen-Rutishauser B, Kuhn DA, Ali Z, Gasser M, Amin F, Parak WJ, et al. Quantification of gold nanoparticle cell uptake under controlled biological conditions and adequate resolution. Nanomedicine (Lond). 2013
20. Carroll RC, Beattie EC, Xia H, Luscher C, Altschuler Y, Nicoll RA, et al. Dynamin-dependent endocytosis of ionotropic glutamate receptors. Proc Natl Acad Sci U S A. 1999; 96:14112–7. [PubMed: 10570207]
21. MacKay JA, Deen DF, Szoka FC Jr. Distribution in brain of liposomes after convection enhanced delivery; modulation by particle charge, particle diameter, and presence of steric coating. Brain Res. 2005; 1035:139–53. [PubMed: 15722054]
22. Vavra M, Ali MJ, Kang EW, Navalitloha Y, Ebert A, Allen CV, et al. Comparative pharmacokinetics of 14C-sucrose in RG-2 rat gliomas after intravenous and convection-enhanced delivery. Neuro-oncol. 2004; 6:104–12. [PubMed: 15134624]
23. Sampson JH, Archer G, Pedain C, Wembacher-Schroder E, Westphal M, Kunwar S, et al. Poor drug distribution as a possible explanation for the results of the PRECISE trial. J Neurosurg. 113:301–9. [PubMed: 20020841]
24. Hadjipanayis CG, Machaidze R, Kaluzova M, Wang L, Schuette AJ, Chen H, et al. EGFRvIII antibody-conjugated iron oxide nanoparticles for magnetic resonance imaging-guided convection-enhanced delivery and targeted therapy of glioblastoma. Cancer Res. 70:6303–12. [PubMed: 20647323]
25. Singh N, Jenkins GJ, Asadi R, Doak SH. Potential toxicity of superparamagnetic iron oxide nanoparticles (SPION). Nano reviews. 2010; 1
26. Hoskins C, Cuschieri A, Wang L. The cytotoxicity of polycationic iron oxide nanoparticles: common endpoint assays and alternative approaches for improved understanding of cellular response mechanism. Journal of nanobiotechnology. 2012; 10:15. [PubMed: 22510488]

27. Gupta AK, Gupta M. Synthesis and surface engineering of iron oxide nanoparticles for biomedical applications. Biomaterials. 2005; 26:3995–4021. [PubMed: 15626447]

28. Muldoon LL, Sandor M, Pinkston KE, Neuwelt EA. Imaging, distribution, and toxicity of superparamagnetic iron oxide magnetic resonance nanoparticles in the rat brain and intracerebral tumor. Neurosurgery. 2005; 57:785–96. discussion 85-96. [PubMed: 16239893]

29. Dickinson PJ, LeCouteur RA, Higgins RJ, Bringas JR, Larson RF, Yamashita Y, et al. Canine spontaneous glioma: a translational model system for convection-enhanced delivery. Neuro Oncol. 12:928–40. [PubMed: 20488958]

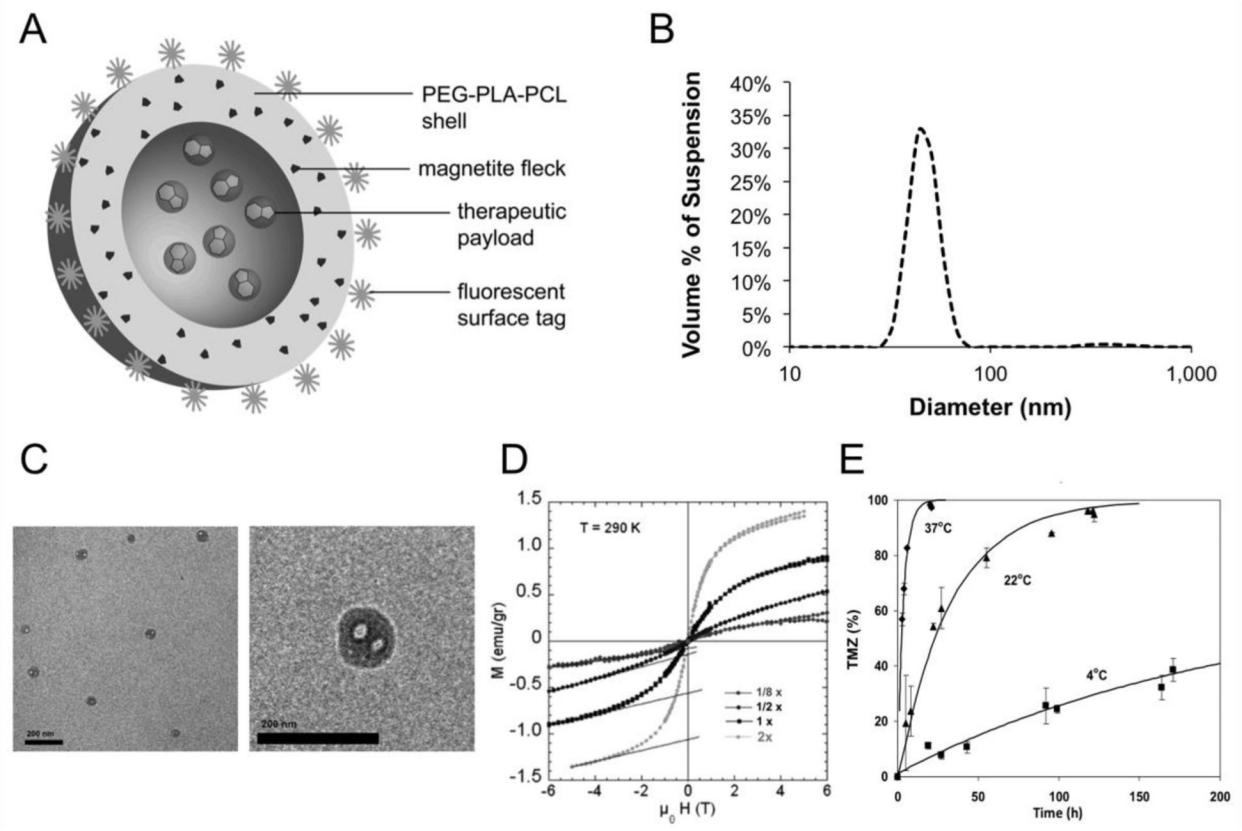

Figure 1. Nanoparticle Characterization

(A) Anatomy of PMNPs fabricated to incorporate superparamagnetic iron oxide (magnetite) into a fluorescently-tagged shell. The payload is protected within the core. (B) Dynamic light scattering (DLS) analysis of PMNPs. (C) Transmission electron microscopy of PMNPs with scale bar set at 200 nm. (D) Magnetic susceptibility of PMNPs with increasing concentrations of magnetite is plotted (1× = 5.5% magnetite). The superparamagnetic behavior is shown in that no hysteresis is apparent as the applied magnetic field is cycled (y axis: applied field and x axis: sample magnetization). (E) Release dynamics of TMZ as assessed by spectrophotometry at the indicated temperature.

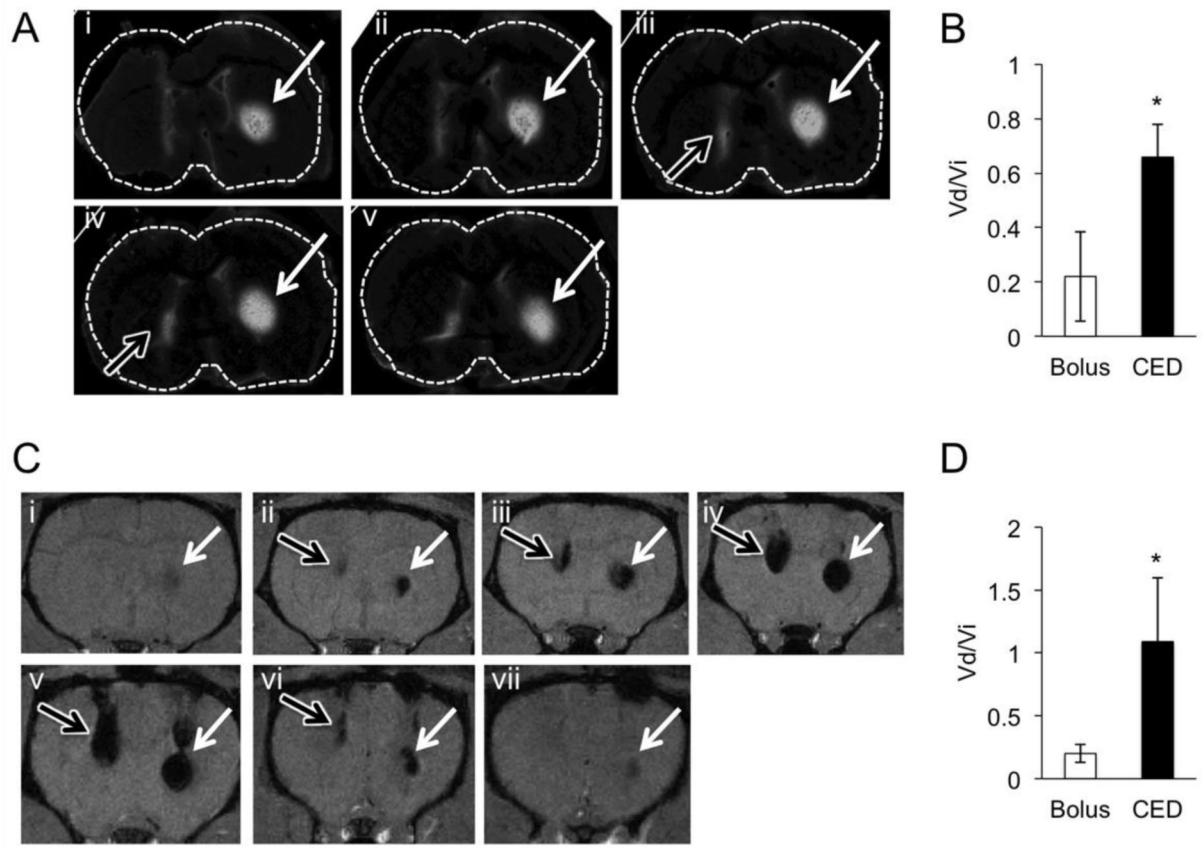

Figure 2. CED increases intracranial distribution of PMNPs

(A) Sequential images of a representative rat brain following infusion of 25 μl PMNPs by CED (white arrows) or bolus injection (black arrows). Slices represent a total of 900 μm in the AP-dimension. (B) Graph of V_d/V_i following infusion of 25 μl of fluorescent PMNPs. Data shows mean value +/− SD. (n = 4 animals per group). * $P < 0.05$. (C) Sequential T2 weighted images following CED (white arrows, right) or bolus infusion (black arrows, left) of 25 μl PMNPs. Slices represent a total of 3.0 mm in the AP-dimension. (D) V_d/V_i following CED or bolus injection as assessed by MRI following infusion of 25 μl PMNPs. (n = 4 animals per group). * $P < 0.05$.

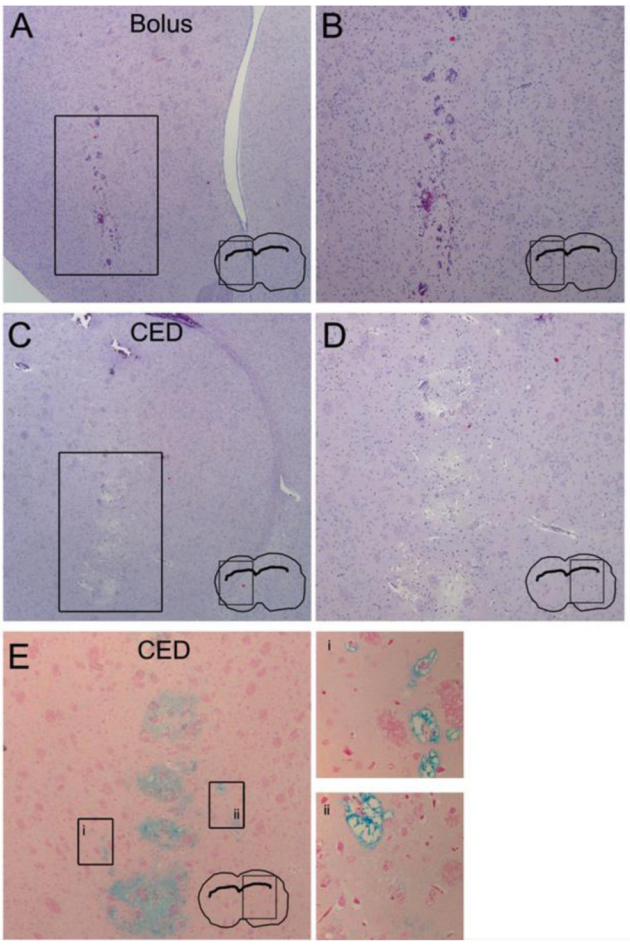

Figure 3. CED of PMNPs does not cause excessive tissue damage

(A-D) Hematoxylin and Eosin stained sections of brain tissue following PMNP infusion. (A and B) Bolus injection of PMNP (magnified insert is shown in B). (C and D) CED infusion (magnified insert is shown in D). (E) Prussian blue staining following PMNP infusion by CED. Boxed areas distant from the infusion site are magnified on the right (inserts i and ii).

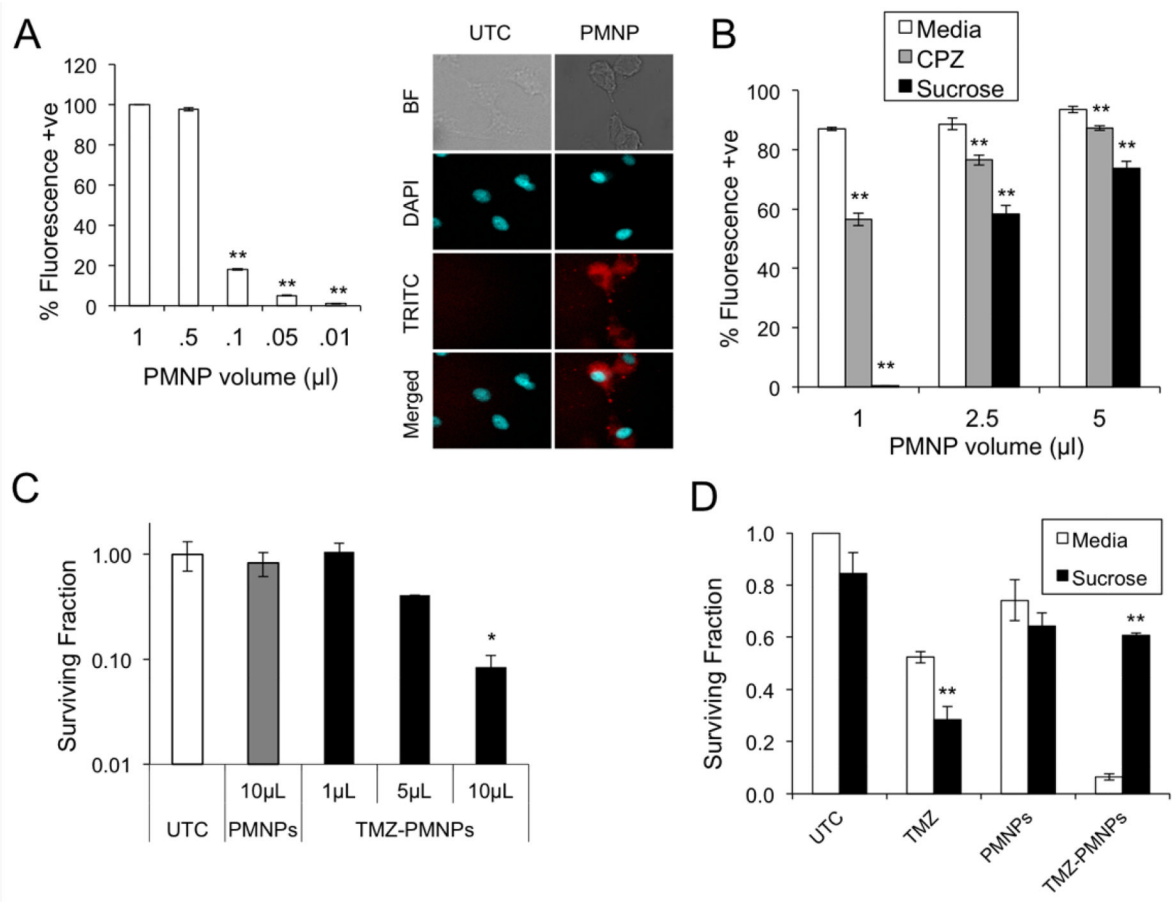

Figure 4. PMNPs are taken up by glioma cells and deliver viable TMZ

(A) Uptake of PMNPs by U87 cells as demonstrated by FACS analysis (left) and confocal imaging (right) following exposure to rhodamine-tagged PMNPs (NP-Rhod) or rhodamine dye alone (UTC) for 2 hours. Rhodamine (TRITC) and nuclei (DAPI) were imaged as shown. (B) FACS analysis of PMNP uptake in the presence of the endocytosis inhibitors, chlorpromazine (30 μM) or hypertonic sucrose (450 mM). (C) Clonogenic assay of U87 cells following treatment with increasing amounts of TMZ loaded PMNPs (TMZ NP) or blank PMNPs. (D) Clonogenic assay of U87 cells, in the presence of 450 mM sucrose or regular media, following treatment with TMZ (50 μM), blank PMNPs, or TMZ-carrying PMNPs (carrying 50 μM TMZ). Clonogenic data show mean surviving fraction, normalized to untreated, of triplicate samples +/− SD. * $P < 0.05$ and ** $P < 0.01$ relative to untreated control.

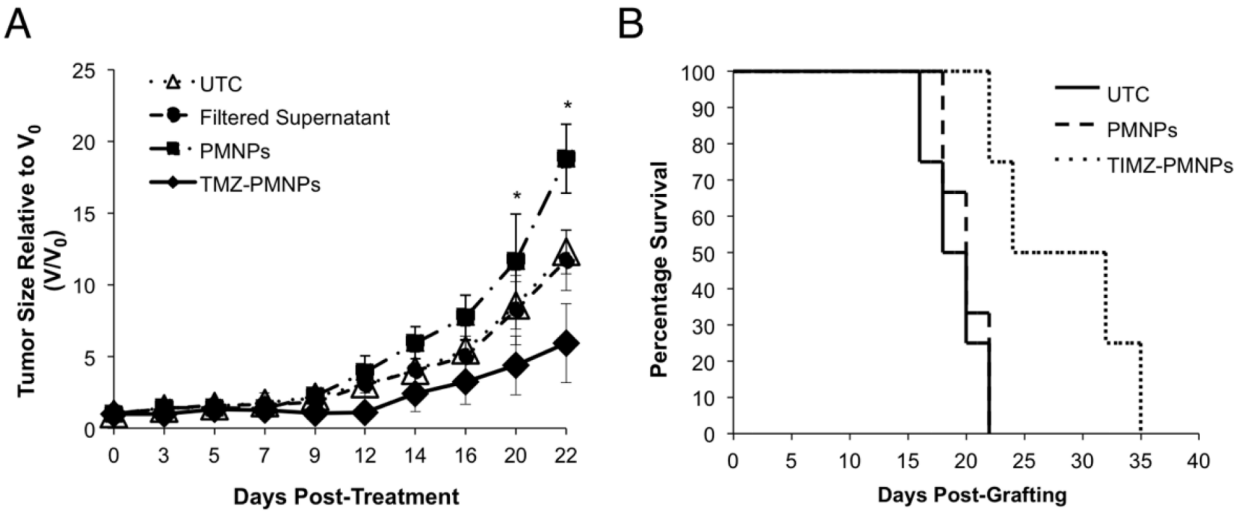

Figure 5. TMZ-PMNPs demonstrate anti-glioma efficacy

(A) U87 hindlimb xenografts were allowed to grow to an average of 200 mm^3 and animals randomized into the groups indicated (n = 5 per group). Graph shows ratio of the tumor volume on any given day (V) relative to the volume of the same tumor on the day treatment was initiated (V_0) +/− SD, following treatment with the indicated PMNP. * $P < 0.05$, TMZ loaded PMNPs (TMZ NP) relative to untreated (UTC). (B) Kaplan-Meier curve of mice bearing intracranial U87 xenografts either untreated or treated with TMZ-PMNPs or Blank-PMNPs. (n = 5 animals per treatment group). $P < 0.03$, TMZ-PMNPs versus Blank-PMNPs.